The paper was presented at the Tenth Meeting
"New Trends in Fatigue and Fracture" (NT2F10)
Metz, France, 30 August–1 September, 2010

Bashir Younise[1], Marko Rakin[2], Nenad Gubeljak[3], Bojan Medjo[2], Aleksandar Sedmak[1]

NUMERICAL SIMULATION OF CONSTRAINT EFFECT ON FRACTURE INITIATION IN WELDED SPECIMENS USING A LOCAL DAMAGE MODEL

NUMERIČKA SIMULACIJA UTICAJA VEZE NA INICIJACIJU LOMA KOD ZAVARENIH EPRUVETA UPOTREBOM MODELA LOKALNOG OŠTEĆENJA

Original scientific paper
UDC: 66.011-034.1 : 519.711-034.1
Paper received: 31.01.2011

Author's address:
[1)] University of Belgrade, Faculty of Mechanical Engineering, Kraljice Marije 16, 11000 Belgrade, Serbia
[2)] University of Belgrade, Faculty of Technology and Metallurgy, Karnegijeva 4, 11000 Belgrade, Serbia
[3)] University of Maribor, Faculty of Mechanical Engineering, Smetanova 17, SI-2000 Maribor, Slovenia

Keywords
- stress triaxiality
- void volume fraction
- ductile fracture
- transferability

Ključne reči
- troosnost napona
- zapreminski udeo šupljine
- duktilan lom
- transferabilnost

Abstract

In this paper, two micromechanical models: the Gurson-Tvergaard-Needleman (GTN) model and Complete Gurson Model (CGM) are used to predict ductile fracture initiation of two different welded specimens, SE(B) and C(T). The effect of strength mismatch and weld metal width on fracture initiation is studied also. High strength low-alloyed (HSLA) steel welded specimens are analysed, with the pre-crack length/specimen width ratio $a_0/W = 0.32$. Two different weld metals with two different widths: 6 and 12 mm are used to make strength overmatch and undermatch joints. Numerical analysis is done previously to adopt Gurson parameters and to determine the values of critical void volume fraction (f_c), which are used in the prediction of crack growth initiation in the two welded specimens. Crack tip opening displacement and J-integral at crack growth initiation ($CTOD_i$ and J_i) are estimated using the GTN and CGM models. Transferability of fracture initiation parameters ($CTOD_i$ and J_i) between the two welded specimens is analysed based on stress triaxiality in front of the crack tip.

Izvod

U ovom radu, primenjena su dva mikromehanička modela: Gurson-Tvergard-Nidlman (GTN) model i Potpuni Gurson model (CGM) za procenu inicijacije duktilnog loma kod dve različite zavarene epruvete, SE(B) i C(T). Uticaj mismečinga čvrstoće i širine metala šava na inicijaciju loma je takođe proučen. Analizirani su zavareni uzorci od niskolegiranog čelika povišene čvrstoće (HSLA), sa izvedenom prslinom, dužina prsline/širina epruvete $a_0/W = 0.32$. Upotrebljena su dva različita metala šava sa dve širine: 6 i 12 mm radi izvođenja overmečing i andermečing spojeva. Prethodno je urađena numerička analiza radi usvajanja Gurson parametara i određivanja vrednosti kritičnog zapreminskog udela šupljine (f_c), koji su iskorišćeni za predviđanje inicijacije rasta prsline u obe zavarene epruvete. Pomeranje pri otvaranju vrha prsline i J integral pri inicijaciji rasta prsline ($CTOD_i$ i J_i) su sračunati prema modelima GTN i CGM. Transferabilnost parametara inicijacije loma ($CTOD_i$ i J_i) između obe zavarene epruvete je analizirana na osnovu troosnosti napona ispred vrha prsline.

INTRODUCTION

Ductile fracture of metallic materials involves micro-void nucleation and growth, and final coalescence of neighbouring voids to create new surfaces of a macro-crack. Local approach has been extensively used in the last decade in order to analyse and predict ductile fracture initiation of alloys. A large number of models have been developed to analyse ductile fracture, these models link material fracture behaviour to the parameters that describe the evolution of micro-voids rather than the conventional global fracture parameters that cannot be directly transferred from one geometry to the other one. Ductile failure process for porous materials is often modelled by means of the Gurson model, /1/, which is one of the most widely known micro-mechanical models for ductile fracture, and describes the progressive degradation of material stress capacity. In this model, which is a modification of the von Mises one, an elastic-plastic matrix material is considered and a new internal variable, the void volume fraction, f, is introduced. The original Gurson model is later modified by many authors, particularly by Tvergaard and Needleman, and is known as the GTN model, /2/.

In this paper, the effect of strength mismatch and width of welded joints on ductile fracture behaviour is investigated

by using two types of welded specimens; single-edge notched bend SE(B), and compact C(T) specimens. The transferability of ductile fracture initiation parameter between two specimens is discussed. The two types of welded specimens made of high strength low alloyed (HSLA) steel are used to analyse the effect of constraint in case of over-matched, OM, and under-matched, UM, welded joints. Micro-mechanical GTN and CGM models are applied in order to predict the crack growth initiation and to analyse the transferability of ductile fracture parameters between welded specimens.

MODELLING OF DUCTILE FRACTURE

Ductile damage develops through three stages: nucleation, growth and coalescence of voids, resulting in final failure, /3/. Growth of nucleated voids strongly depends on stress and strain state. Most experiments and analyses show an exponential increase with the stress triaxiality, which is defined as the ratio of mean stress, σ_m, to equivalent stress, σ_{eq}. Ductile fracture models may be classified in two groups: uncoupled micro-mechanical models, and coupled micro-mechanical models. In uncoupled modelling, void presence does not significantly alter the behaviour of the material, /4/, so the model does not include the damage parameter and the von Mises criterion is most frequently used as a yield criterion, while the coupled micro-mechanical model considers the material as a porous medium where the influence of nucleated voids on the stress-strain state and plastic flow can not be avoided. The GTN model is based on the hypothesis that void nucleation and growth in a metal may be macroscopically described by extending the von Mises plasticity theory to cover the effects of porosity occurring in the material. The void volume fraction, f, as a variable is introduced into the expression for the plastic potential, /1/:

$$\phi=\frac{3S_{ij}S_{ij}}{2\sigma_{eq}^2}+2q_1f^*\cosh\left(\frac{3q_2\sigma_m}{2\sigma_{eq}}\right)-\left[1+(q_1f^*)^2\right]=0 \quad (1)$$

where σ_{eq} denotes the yield stress of the material matrix, σ_m is mean stress, S_{ij} is the stress deviator, the parameters q_1 and q_2 are introduced by Tvergaard, /5/, to improve the ductile fracture prediction of the Gurson model and f^* is the damage function, /2/:

$$f^*=\begin{cases} f & for \quad f\le f_c \\ f_c+K(f-f_c) & for \quad f>f_c \end{cases} \quad (2)$$

where f_c is the critical void volume fraction at the moment when void coalescence occurs. The parameter K defines the slope of sudden drop of the force on the force-diameter reduction diagram.

In ductile steel, the voids nucleate due to separation or fracture of non-metallic inclusions and secondary-phase particles from the material matrix. Two phenomena contribute to the increase of void volume fraction in FE analysis with the embedded GTN yield criterion: one is the growth of the existing voids and the other is the nucleation of new voids under external loading:

$$\dot f=\dot f_{nucleation}+\dot f_{growth} \quad (3)$$

$$\dot f_{nucleation}=A\dot\varepsilon_{eq}^p \quad (4)$$

$$\dot f_{growth}=(1-f)\dot\varepsilon_{ii}^p \quad (5)$$

where $\dot\varepsilon_{eq}^p$ is the equivalent plastic strain rate, $\dot\varepsilon_{ii}^p$ is the plastic part of the strain rate tensor and A is concerning to the model proposed by Chu and Needleman, /6/, for modelling nucleation of secondary voids, based on normal distribution:

$$A=\frac{f_N}{S_N\sqrt{2\pi}}\exp\left[-\frac{1}{2}\left(\frac{\varepsilon_{eq}-\varepsilon_N}{S_N}\right)^2\right] \quad (6)$$

where f_N is the volume fraction of secondary void-forming particles, ε_N is the mean strain corresponding to the nucleation of voids, and S_N is the corresponding standard deviation.

The description of the coalescence of voids can be improved by using the model of plastic limit load proposed by Thomason, /3/, and analysing the localized deformation state in ligaments between the voids. Zhang, et al. /12/ made a significant modification of the GTN model; they applied the Thomason void-coalescence criterion, thus introducing the Complete Gurson Model (CGM). The criterion for determining the time when the void coalescence begins is expressed by the ratio of the maximum principle stress to the actual yield stress:

$$\frac{\sigma_1}{\bar\sigma}>\left[\alpha\left(\frac{1}{r}-1\right)+\frac{\beta}{\sqrt{r}}\right](1-\pi r^2) \quad (7)$$

where α and β are constants, /3/, and r is the void space ratio given by the formula:

$$r=\left(\frac{3f}{4\pi}e^{\varepsilon_1+\varepsilon_2+\varepsilon_3}\right)^{1/3}\left(\frac{\sqrt{e^{\varepsilon_2+\varepsilon_3}}}{2}\right)^{-1} \quad (8)$$

where ε_1, ε_2 and ε_3 are the principle strains. In the CGM, the critical void volume fraction f_c is the response of material to the coalescence of voids but it is not a material constant as in the GTN model.

The critical void volume fraction f_c, determined on a round smooth specimen in the GTN model, is used to predict the onset of crack growth on single-edge notched bend SE(B), and on compact C(T) specimens, while f_c in the CGM model is determined by the user material subroutine, based on /12/.

MATERIALS AND EXPERIMENTAL PROCEDURE

The base metal (BM) made of high strength low alloyed (HSLA) steel is used in a quenched and tempered condition. The fluxed-cored arc welding (FCAW) process in shielding gas is used and two different fillers are used to produce over-matching (OM) and under-matching (UM) weld metal. The mechanical properties and chemical composition of used materials are given in Tables 1 and 2, respectively. The mismatching factor M is defined as:

$$M=\frac{R_{P0.2WM}}{R_{P0.2BM}} \quad (9)$$

where $R_{p0.2WM}$, and $R_{p0.2BM}$ are yield stresses of weld and base metals, in respect.

Table 1. Mechanical properties of BM and WMs at room temperature.
Tabela 1. Mehaničke osobine OM i MŠ na sobnoj temperaturi.

Material	E (GPa)	$R_{p0.2}$ (MPa)	R_m (MPa)	M
Over-matching	183.8	648	744	1.19
Base metal	202.9	545	648	–
Under-matching	206.7	469	590	0.86

Table 2. Chemical composition of base metal and fillers in weight %.
Tabela 2. Hemijski sastav osnovnog i dodatnog materijala u tež. %

Material	C	Si	Mn	P	S	Cr	Mo	Ni
Filler-OM	0.04	0.16	0.95	0.01	0.02	0.49	0.42	2.06
Base metal	0.123	0.33	0.56	0.003	0.002	0.57	0.34	0.13
Filler-UM	0.096	0.58	1.24	0.013	0.16	0.07	0.02	0.03

The damage parameters of materials such as; initial void volume fraction, f_0, for non-metallic inclusions and mean free path, λ, between non-metallic inclusions are adopted in /8/. The effect of secondary voids on ductile fracture is neglected as based on that these secondary voids formed around Fe_3C particles have extremely low effect and are present only during the final stage of ductile fracture, /8/.

The critical void volume fraction values, f_c, (Table 3) in the GTN model are determined by combined experimental-numerical results from void volume fraction – round tensile (RT) diameter reduction curve. The value of critical void fraction, f_c, is determined corresponding to the experimental diameter reduction at final fracture, /7/. The Gurson parameters of HSLA steel are given in Table 3 for over-matched (OM), and under-matched (UM) weld metal.

Table 3. Gurson parameters of HSLA steel.
Tabela 3. Gurson parametri za HSLA čelik.

Material	f_0	f_c	q_1	q_2
OM-WM	0.002	0.0173	1.5	1
UM-WM	0.002	0.0238	1.5	1

Mechanical tests are conducted at room temperature. True stress-true strain diagrams are shown in Fig. 1. Two welded joints (SE(B) and C(T) specimens) are used, Figs. 2 and 3.

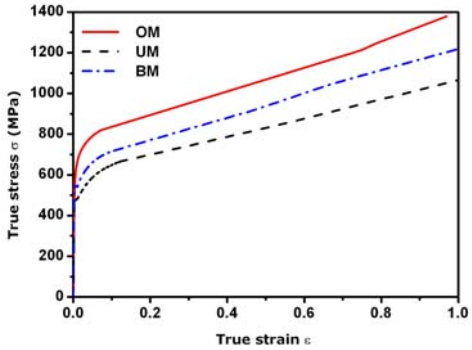

Figure 1. True stress–true strain curves of used materials.
Slika 1. Krive stvarni napon–deformacija upotrebljenih materijala.

The geometry of SE(B) is given in /7/. The SE(B) specimen is fatigue precracked and the ratio of crack length to specimen width is $a_0/W = 0.32$ for both specimens.

Welded joints are considered as bimaterial joints, since the crack is located in the weld metal along the axis of symmetry of the weld. Two different widths of weld metal for both OM and UM welded joints are used: $2H = 6$ and 12 mm as shown in Figs. 2 and 3.

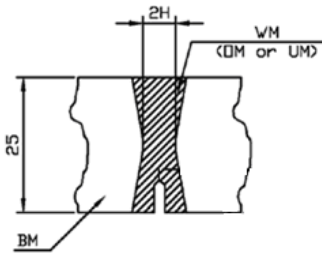

Figure 2. Welded joint of SE(B) specimen.
Slika 2. Zavareni spoj epruvete SE(B).

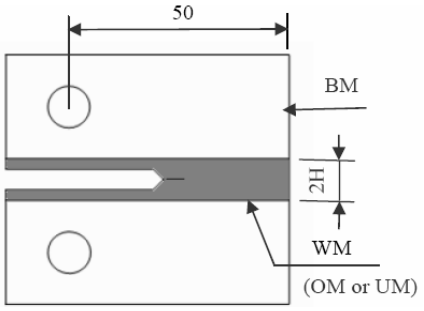

Figure 3. Geometry of welded C(T) specimen.
Slika 3. Geometrija zavarene epruvete C(T).

NUMERICAL MODELLING OF WELDED SPECIMENS

The finite element modelling (FEM) programme (ABAQUS) is used with the integrated yield criterion for determination of the value of stress and strain components and the value of f at non-linear behaviour. The specimens are analysed under plane-strain conditions, and 8-noded isoparameteric reduced integration elements are used, /10, 11/.

FE mesh size (0.15×0.15 mm) of SE(B) and C(T) specimens approximates to the estimated value of the mean free path λ between non-metallic inclusions. Figure 4 shows FE mesh of C(T) specimen with magnification of the mesh near the crack tip, while FE mesh of SE(B) specimen is given in /7/. Due to the symmetry of SE(B) and C(T) specimens, half of the specimens are modelled.

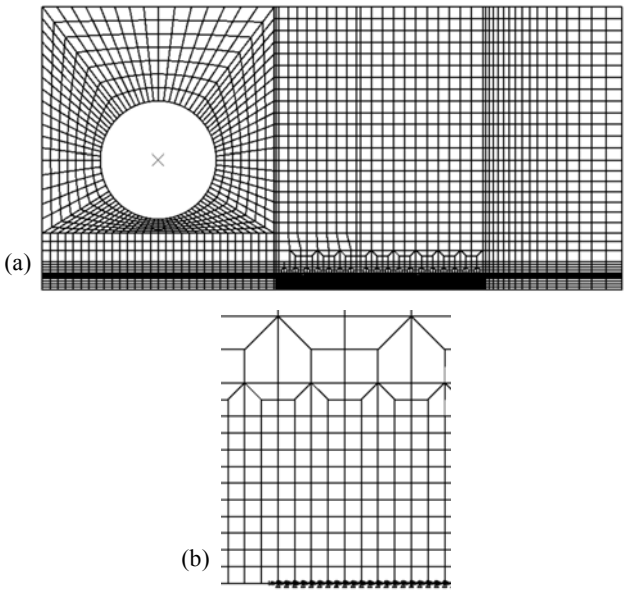

Figure 4. FE mesh of C(T) specimen (a); detail of crack-tip mesh (b).
Slika 4. Mreža FE epruvete C(T) (a); detalj mreže vrha prsline (b).

RESULTS AND DISCUSSION

Prediction of crack growth initiation

The values of critical void volume fraction, f_c, in both models are used for prediction of crack growth initiation on SE(B) and C(T) specimens. Crack growth initiation on a pre-cracked geometry is defined by the instant when the first element in front of the crack tip becomes damaged.

It is shown in /8/ that the condition for the onset of crack growth, as determined by the J-integral at initiation, J_i, is most adequately defined by the micro-mechanical criterion:

$$f \geq f_c \tag{10}$$

The onset of crack growth occurs when the condition given by Eq. (10) is satisfied. Crack growth initiation described here by crack tip opening displacement ($CTOD_i$) at crack growth initiation and J-integral (J_i) at crack growth initiation is determined using GTN and CGM models for OM and UM weld metals on SE(B) and C(T) specimens, that corresponds to critical void volume fraction, f_c (Figs. 5, 6, 7, 8, 9 and 10). The experimentally and numerically obtained values of $CTOD_i$ using both models for OM and UM weld metal in case of 6 and 12 mm weld metal widths on SE(B) and C(T) specimens are given in Table 4. As can be seen from Table 4, the values of $CTOD_i$ for the C(T) specimen are more conservative than the values of the SE(B) specimen. The results of SE(B) specimen are in good agreement with experimental data in case of UM specially determined by the CGM model that due to CGM model does not use a constant f_c as in the GTN model, but in case of OM joints, there are some deviations which may be due to a small fraction of cleavage occurring in the welded joint /7/. Moreover, the effect of strength mismatching and the width of weld metal can be predicted successfully by using GTN and CGM models. It is noticeable also by using both models: the higher resistance to ductile fracture initiation is attained in OM welded joints with smaller width of weld metal, while the resistance to ductile fracture initiation of UM welded joints increases with the increase in width of the weld metal, these obtained results are in agreement with the experimental results given in /12/.

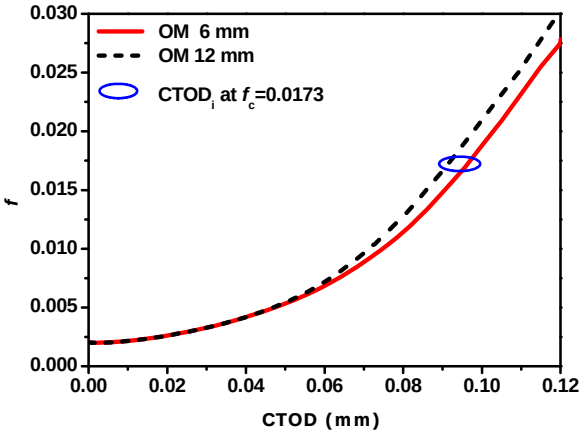

Figure 5. Void volume fraction f vs. crack tip opening displacement CTOD by GTN model for C(T) specimen with two different widths of OM weld metal.
Slika 5. Zapreminski udeo šupljine f u funkciji CTOD prema modelu GTN za epruvetu C(T) sa dve različite širine OM metala šava.

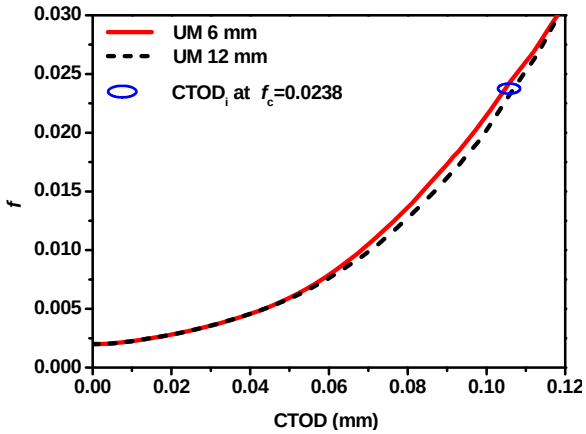

Figure 6. Void volume fraction f vs. crack tip opening displacement CTOD by GTN model for C(T) specimen with two different widths of UM weld metal.
Slika 6. Zapreminski udeo šupljine f u funkciji CTOD prema modelu GTN za epruvetu C(T) sa dve različite širine UM metala šava.

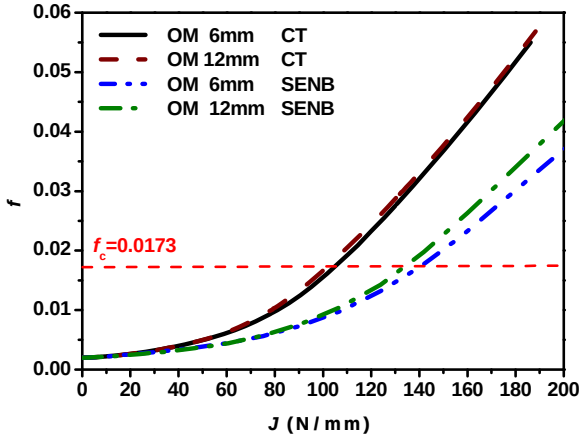

Figure 7. Void volume fraction f vs. J-integral by GTN model for SE(B) and C(T) specs. with two different widths of OM weld metal.
Slika 7. Zapreminski udeo šupljine f u funkciji J integrala prema modelu GTN za epruvete SE(B) i C(T) sa dve različite širine OM metala šava.

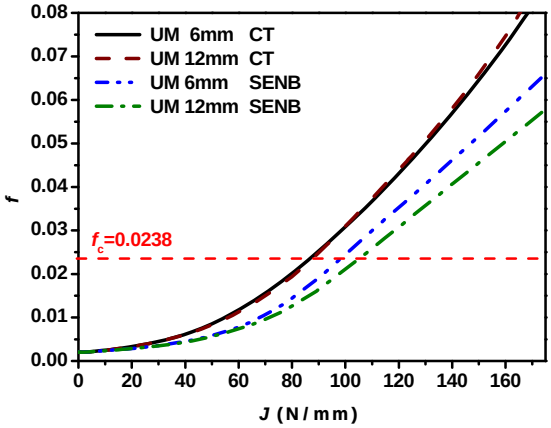

Figure 8. Void volume fraction f vs. J-integral by GTN model for SE(B) and C(T) specs. with two different widths of UM weld metal.
Slika 8. Zapreminski udeo šupljine f u funkciji J integrala prema modelu GTN za epruvete SE(B) i C(T) sa dve različite širine UM metala šava.

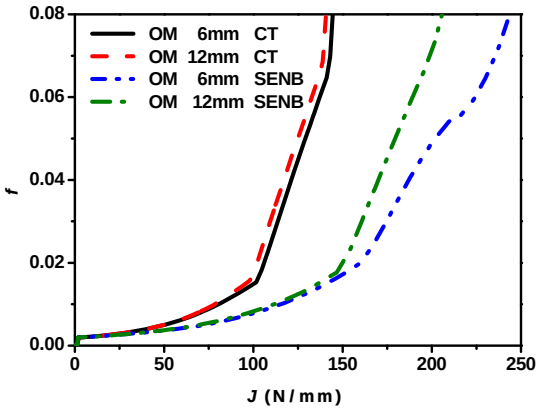

Figure 9. Void volume fraction *f* vs. J-integral by CGM model for SE(B) and C(T) specimens with two different widths of OM WM.
Slika 9. Zapreminski udeo šupljine *f* u funkciji J integrala prema modelu CGM za epruvete SE(B) i C(T) sa dve različite širine OM.

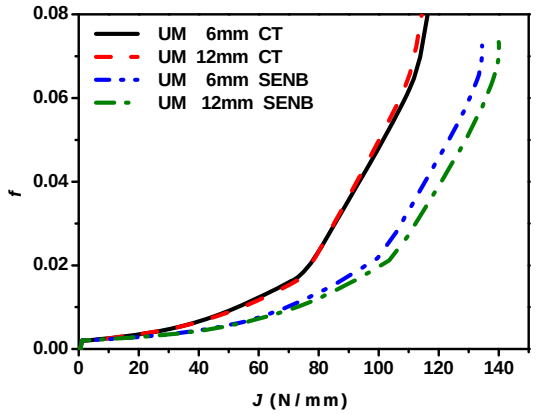

Figure 10. Void volume fraction *f* vs. J-integral by CGM model for SE(B) and C(T) specimens with two different widths of UM weld metal.
Slika 10. Zapreminski udeo šupljine *f* u funkciji J integrala prema modelu CGM za epruvete SE(B) i C(T) sa dve različite širine UM metala šava.

Table 4. Experimental and numerical values of $CTOD_i$ for SE(B) and C(T) specimens in case of OM and UM.
Tabela 4. Eksperimentalni i numerički rezultati za $CTOD_i$ za SE(B) i C(T) epruvete za slučajeve OM i UM.

Specimen type		$CTOD_i$ (mm)					
		$2H$ = 6 mm			$2H$ = 12 mm		
		Exper.	Num. GTN	Num. CGM	Exper.	Num. GTN	Num. CGM
SE(B)	OM	0.092	0.110	0.157	0.084	0.106	0.137
	UM	0.120	0.124	0.119	0.124	0.129	0.129
C(T)	OM	–	0.097	0.094	–	0.092	0.088
	UM	–	0.105	0.086	–	0.107	0.090

Corresponding crack growth initiation values of the J-integral (J_i) to $CTOD_i$ are numerically determined using both models for C(T) and SE(B) specimens and the values are given in Table 5. It is noticeable also from Table 5 that the highest resistance to ductile fracture initiation is attained in OM welded joints with the smallest width of the weld metal, while the resistance to ductile facture initiation of UM welded joints increases with the increase of width of the weld metal. These obtained results are in agreement with the experimental analysis given in /12/.

Table 5. Numerical results of J_i corresponding to $CTOD_i$ for SE(B) and C(T) specimens: OM and UM.
Tabela 5. Numerički rezultati J_i koji odgovaraju $CTOD_i$ za SE(B) i C(T) epruvete: OM i UM.

Specimen type		J_i (N/mm)			
		$2H$ = 6 mm		$2H$ = 12 mm	
		GTN	CGM	GTN	CGM
SE(B)	OM	142.1	160.0	135.4	146.8
	UM	97.3	99.5	107.2	103.5
C(T)	OM	105.6	101.6	102.2	98.2
	UM	87.4	72.1	88.1	73.0

EVALUATION OF CONSTRAINT LEVEL IN WELDED SPECIMENS

In the present investigation, the constraint levels based on stress triaxiality are compared along ligament. Figures 11, 12 and 13 illustrate the variation of stress triaxility due to the variation of specimen geometry with loading condition, strength mismatching and width of weld metal, respectively. One can notice from Fig. 11 that the stress triaxiality level of C(T) specimen at crack tip is higher than the stress triaxiality of SE(B) specimen, therefore, the values of $CTOD_i$ for C(T) specimen are smaller than the values of SE(B) specimen in cases of OM and UM. It is noticeable also in Figs. 11, 12 and 13, that the most influence on stress triaxiality at crack growth initiation is dominant for the specimen geometry with the loading condition, strength mismatching and weld metal width, respectively.

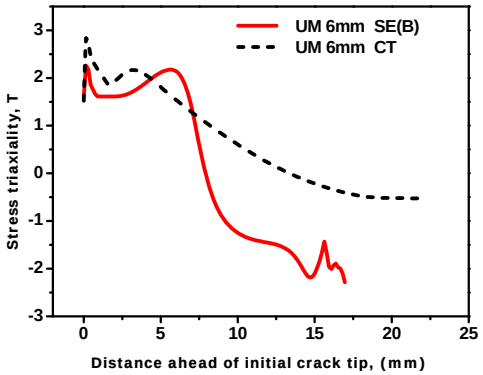

Figure 11. Variation of stress triaxiality along ligament due to variation of specimen geometry with loading condition – UM.
Slika 11. Promena troosnosti napona duž ligamenta usled promene geometrije epruvete u uslovima opterećenja za UM.

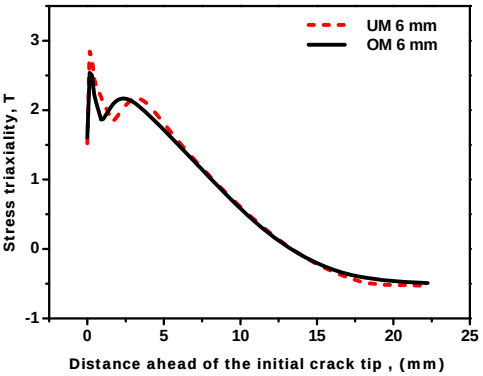

Figure 12. Variation of stress triaxiality along ligament due to variation of strength mismatching for C(T) specimen.
Slika 12. Promena troosnosti napona duž ligamenta usled promene čvrstoće mismečinga za C(T) epruvetu.

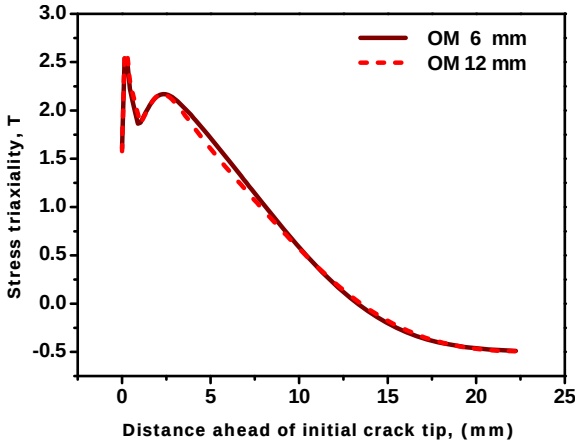

Figure 13. Variation of stress triaxiality along ligament due to variation of width of weld metal for C(T) specimen.
Slika 13. Promena troosnosti napona duž ligamenta usled promene širine metala šava za C(T) epruvetu.

Figure 14 illustrates the higher opening stress, σ_{22}, at initiation for C(T) specimen compared to the SE(B) specimen due to the effect of constraint. From the available literature, /11/, based on quantifying the level of constraint, if the triaxial conditions are found to be similar, then it is believed that crack growth initiation values $CTOD_i$ are transferable within certain circumstances. These conditions are evident for the geometries where the ligament length is large in the case of bending geometries and geometries that are predominately under tension. To compare the stress triaxiality of the specimen and components, one should take into account the remaining ligament which should be considered for comparison, some investigations, /13/, indicate that the critical distance from the crack tip, where cleavage fracture initiation occurs, is within the range of J/σ_0 to $5J/\sigma_0$ (J is the J-integral and σ_0 is the yield stress), therefore, the proper specimens for structural integrity assessment can be selected according to constraint level, if the constraint level of the specimen matches the constraint level of the component, the results of the specimen seem to be transferred to that component within certain circumstances.

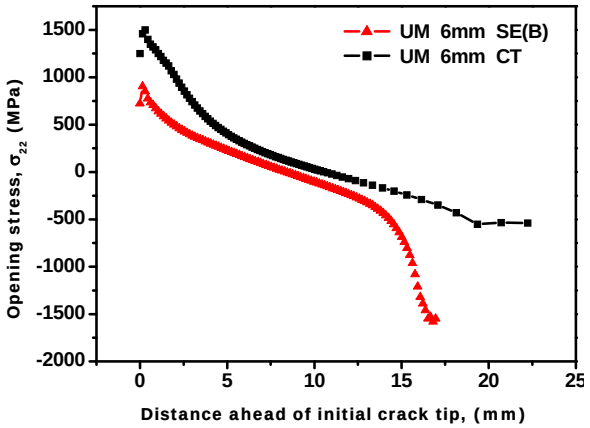

Figure 14. Opening stress ahead of initial crack tip for SE(B) and C(T) specimens in case of 6 mm weld metal width, UM.
Slika 14. Napon otvaranja ispred vrha inicijalne prsline za epruvete SE(B) i C(T) za slučaj širine metala šava 6 mm, UM.

CONCLUSION

Ductile fracture initiation of welded specimens made of high strength low alloyed steel is investigated by using micromechanical GTN and CGM models. SE(B) and C(T) welded specimens are used to analyse ductile fracture behaviour by predicting crack growth initiation and the effect of constraint level. The transferability of results from one component to another is analysed based on stress triaxiality to find a way how ductile fracture parameters can be transferred from specimens to components. One can conclude: GTN and CGM models can predict ductile fracture initiation $CTOD_i$ of welded specimens and the effect of constraint level based on critical void volume fraction, f_c, and the highest influence of constraint on stress triaxiality at crack growth initiation is for specimen geometry with loading condition, strength mismatching, and weld metal width, respectively. Ductile fracture initiation parameters such as $CTOD_i$ and J_i can be transferred from a component to another within certain circumstances if their triaxial conditions are similar, therefore, to transfer ductile fracture parameters from specimens to components, one should choose the proper specimen which has a constraint level similar to the component.

REFERENCES

1. Gurson, A., *Continuum theory of ductile rupture by void nucleation and growth, part I:. yield criteria and flow rules for porous ductile media*, J Engng Mater Tech. 1977; 99 : pp.2-15.
2. Tvergaard, V., Needleman, A., *Analysis of cup-cone fracture in a round tensile bar*, Acta metal 1984; 32 : pp.57-169.
3. Thomason, P.F., Ductile fracture of metals, Pergamon Press, Oxford, 1990.
4. Bauvineau, L., Burlet, H., Eripret, C., Pineau, A., *Modelling of ductile stable crack growth in a C-Mn steel with local approach*, Paris, 1996, pp.22-32.
5. Tvergaard, V., *Influence of voids on shear bands instabilities under plane strain conditions*, Int. J. Fract., 1981; 17 : pp.389-407.
6. Chu, C., Needleman, A., *Void nucleation effects in biaxiality stretched sheets*, J. Engng Mater. Technol., 1980; 102: pp.249-256.
7. Zhang, Z.L., Thaulow, C., Odegard, J., *A complete Gurson model approach for ductile fracture*, Eng. Fract. Mech., 2000, 67, No.2, pp.155-168.
8. Rakin, M., Gubeljek, N., Dobrojevic, M., Sedmak, A., *Modelling of ductile fracture initiation in strength mismatched welded joint*, Engng Fract. Mech. 2008; pp.3499-3510.
9. Rakin, M., Cvijovic, Z., Grabulov, V., Putic, S., Sedmak, A., *Prediction of ductile fracture initiation using micro-mechanical analysis*, Engng Fract. Mech. 2004; 71: pp.813-827.
10. Berković, M., *Determination of Stress Intensity Factors Using Finite Element Method*, Structural Integrity and Life, Vol.4, No2 (2004), pp.57-62.
11. Berković, M., *Numerical Methods in Fracture Mechanics*, Struct. Int. and Life, Vol.4, No2 (2004), pp.63-66.
12. Gubeljak, N., Scheider, I., Kocak, M., Predan, J., *Constraint effect on fracture behaviour or strength mismatched weld joint*, 14 Europ. Conf. on Frac., EMAS publishing; 2002. pp.647-655.
13. Parankumar, T.V., Chattopadhyay, J., Dutta, B.K., Kushwaha, H.S., *Transferability of specimen J-R curve to straight pipes with through-wall circumferential flaws*, Pressure Vessel and Piping, 2002; 79: pp.127-134.